



|              |   |
|--------------|---|
| Title        | Experiment and numerical simulation in temperature distribution and welding distortion in GMA welding |
| Author(s)    | Yamane, Satoshi; Yamazaki, Takuya; Kaneta, Tomoaki et al.   |
| Citation     | Transactions of JWRI. 2010, 39(2), p. 190-192   |
| Version Type | VoR   |
| URL          | <a href="https://doi.org/10.18910/5377">https://doi.org/10.18910/5377</a>                             |
| rights       |   |
| Note         |   |

*The University of Osaka Institutional Knowledge Archive : OUKA*

<https://ir.library.osaka-u.ac.jp/>

The University of Osaka

# Experiment and numerical simulation in temperature distribution and welding distortion in GMA welding<sup>†</sup>

YAMANE Satoshi \*, YAMAZAKI Takuya \*, KANETA Tomoaki \*, NAKAJIMA Toru \*\* and  
YAMAMOTO Hikaru \*\*

**KEY WORDS:** (Weld pool) (Numerical simulation) (Welding distortion) (Penetration depth) (Thermal conductivity) (GMA welding) (Temperature distribution of base metal) (Robotic welding) (CAD)

## 1. Introduction

Recently, the robotic welding is applied in the need field to save the human costs and to reduce the need for skilled workers. This is important to save the production costs. If the welding distortion before the welding can be predicted, the design cost will be saved.

The simulation technologies are developed according to the development of computers. In many applications, the numerical simulation is applied to save costs. In the field of the welding, the numerical simulations were proposed and applied to the practical field to determine the welding conditions.

The accuracy of dimensions after welding of the steel structure becomes an important factor for the product cost. The dimension becomes inaccurate due to the welding distortion. Therefore, the control of the welding distortion is demanded in the steel structure welding to improve the productivity. For this purpose, the estimation of the amount of the deformation is needed and its behavior is investigated.

In this paper, the numerical model of the heat source was proposed for the GMA welding. The fundamental welding experiments in the bead were carried out to improve the accuracy of the numerical model. Its model was based on the fundamental welding result and the cross section agreed with the experimental results. During the welding, the behavior of the deformation and the temperature distribution was investigated by using a laser sensor and a thermoelectric couple. Dynamic behavior of the deformation was investigated during the welding. The visualizations of the dynamic behavior of deformation were tried by using the numerical analysis. The behaviors are in good agreement with the experimental results. The effect of the bead shape on the deformation was discussed.

## 2. Fundamental experiment

Setting of the fundamental experiment is shown in Fig. 1. The dimension of the base metal is 500mm length, 200mm width and 12mm thickness. The fundamental experiment was carried out under the conventional welding condition, i.e., setting of the welding voltage, the welding

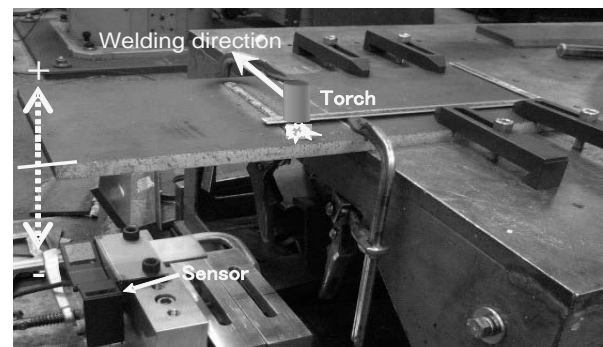


Fig. 1 Setting for fundamental experiment

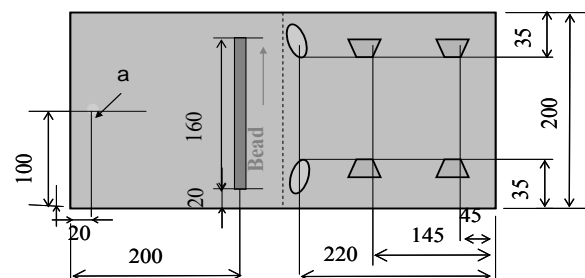


Fig. 2 Clamp position on base metal

Table 1 Parameters in the numerical simulations

|   |                          |
|---|--------------------------|
| Specific heat $c$ [J/kg·K]                      | 473                      |
| Mass density $\rho$ [kg/m <sup>3</sup> ]        | 7850                     |
| Thermal conductivity $\kappa$ [W/m·K]           | 51.5                     |
| Emission coefficient $h$ [W/ m <sup>2</sup> ·K] | 33.4                     |
| Poisson's ratio                                 | 0.33                     |
| Coefficient of linear thermal expansion [1/K]   | 11.8<br>$\times 10^{-6}$ |

current and the welding speed were 28.7 V, 292.6 A and 5 mm/s, respectively. The displacement at the point a in Fig. 2 was measured with a laser displacement meter. The right side of the base metal was restricted by 6 clamps. The numerical model was introduced by using the welding

<sup>†</sup> Received on 30 September 2010

\* Graduate School, Saitama University, Saitama, Japan

\*\* Hitachi Construction Machinery Co., Ltd, Ibaraki, Japan

Transactions of JWRI is published by Joining and Welding Research Institute, Osaka University, Ibaraki, Osaka 567-0047, Japan

conditions.

### 3. Numerical model of welding

Dimension of the numerical model is the same as the fundamental experiment. The flow of the weld pool was neglected. The arc was approximated by the heat input. The numerical model is induced with the assumption, that the heat conduction is dominant. The heat input is equal to the product of the welding voltage  $V$  and the welding current  $I$ . The calculation was carried out under the assumption that 40% of the heat input was used for melting of the electrode wire, i.e., 60% of  $VI$  was given to the base metal. Let heat efficiency to the base metal,  $\eta$ , be 0.7. The heat input  $VI$  is 8400 J/s. An equation of heat conduction is

$$\rho c \frac{\partial U}{\partial t} = \kappa \left( \frac{\partial^2 U}{\partial x^2} + \frac{\partial^2 U}{\partial y^2} + \frac{\partial^2 U}{\partial z^2} \right) \quad (1)$$

where  $\kappa, \rho$  and  $c$  are heat conductivity, density and specific heat, respectively.

The distortion analysis is based on the following partial differential equation:

$$\nabla^2(u, v, w) + \frac{1}{1-2\nu} \left( \frac{\partial e}{\partial x}, \frac{\partial e}{\partial y}, \frac{\partial e}{\partial z} \right) = \frac{2(1+\nu)}{1-2\nu} \alpha \left( \frac{\partial T}{\partial x}, \frac{\partial T}{\partial y}, \frac{\partial T}{\partial z} \right)$$

$$e = \varepsilon_x + \varepsilon_y + \varepsilon_z, \quad \varepsilon_x = \frac{\partial u}{\partial x}, \quad \varepsilon_y = \frac{\partial v}{\partial y}, \quad \varepsilon_z = \frac{\partial w}{\partial z} \quad (2)$$

where  $\nu$  and  $\alpha$  are Poisson's ratio and the coefficient of linear thermal expansion.

The authors tried to denote the latent heat in the numerical simulation, i.e., the specific heat is changed between 1807 K and 1809 K to denote transition temperature between solid and liquid phase. The parameters were listed on Table 1.

### 4. Boundary conditions in numerical model

The Newton cooling law was applied on the surface except for that in contact with the carrier.

$$\rho c \frac{\partial U}{\partial t} = q = -h(u - 293) \quad (3)$$

Since the heat capacity of the carrier is very big, the temperature for the surface in contact with the carrier is fixed to 293 K corresponding to the atmosphere temperature. The heat input to the base metal is divided to two parts, to be agreement with the penetration of the weld pool, as shown in **Fig. 3**. One is the heat input for the base metal. Other one is heat input for the weld pool.

The heat input is denoted by the following equation:

$$q_1(x, y, z) = \frac{3Q}{\pi r^2} \exp\left(\frac{-3x^2}{r^2}\right) \exp\left(\frac{-3z^2}{r^2}\right) \quad (4)$$

where  $r$  is the radius of the heat input to be 6.6 mm.

### 5. Simulation result

Numerical simulation was carried out by FEM, for which the software is Mentat 2007. According to the movement of the heat, the weld pool corresponding to a gray color is moved and the deposited metal was made, as shown in **Fig. 4(a)**. The displacement is denoted as shown

in **Fig. 4(b)**. The left side of the base metal without the clamping was bended.

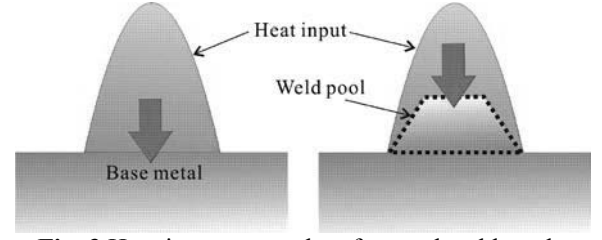


**Fig. 3** Heat input to metal surface and weld pool

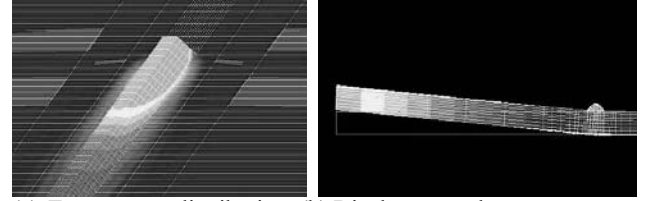


**Fig. 4** Simulation result

The penetration depth and the displacement were compared between the simulation and the fundamental experiment, as shown in **Fig. 5** and **6**.

The simulation results of the bead width and the penetration depth was agreed with the fundamental experimental result. In the fundamental experiment, the displacement was measured with a laser displacement meter. The behavior of the displacement at the point a on the base metal, as shown in **Fig. 1**, is shown in **Fig. 6**. A good agreement between the simulation and the experiment was obtained.

Moreover, the other experiment with other welding conditions was carried out to confirm the validity of the numerical simulation. The results of simulation and the experiment are shown in **Fig. 7** and **8**, respectively.

### 6. Conclusions

The numerical model was designed to investigate the dynamic behavior of the displacement due to the welding distortion. In spite of the difference between the numerical simulations and the experiments about the temperature behavior on the back side of the base metal, the behavior of the displacement in simulation due to the welding distortion almost agreed with experiment.

If the penetration shape in the numerical simulation is the same as the experiment, the welding distortion can be predicted.

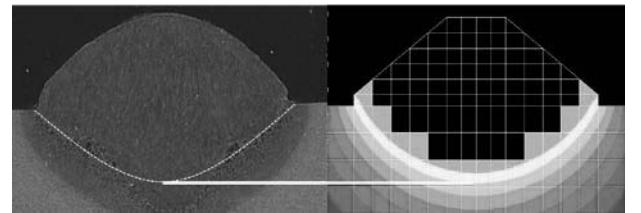


**Fig. 5** Comparison of penetration shape in fundamental experiment

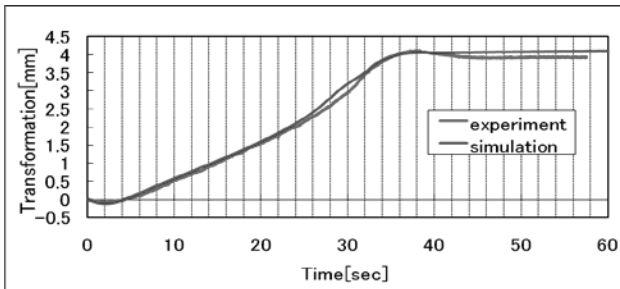


**Fig. 6** Comparison of amounts of transformation in fundamental experiment.

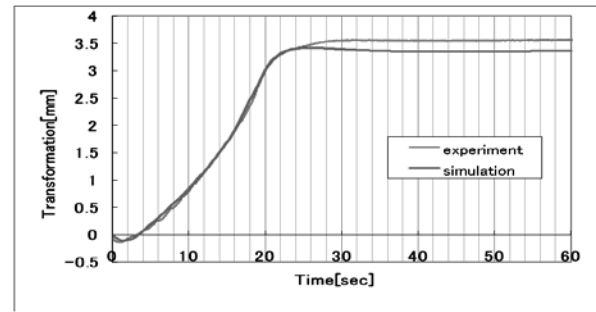


**Fig. 8** Comparison of amounts of transformation.

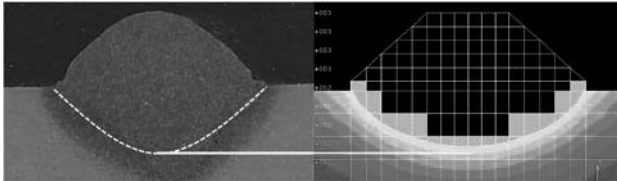


**Fig. 7** Comparison of penetration shape for vilification.